J Electroceram (2010) 24:214–218
DOI 10.1007/s10832-008-9560-9

Fabrication of sub 50-nm direct-patterned $Pb(Zr,Ti)O_3$ films by electron beam-induced metal-organic deposition

Hyeong-Ho Park · Hong-Sub Lee · Hyung-Ho Park · Xin Zhang · Ross H. Hill

Received: 24 September 2008 / Accepted: 10 December 2008 / Published online: 8 January 2009

Abstract Direct-patterned lead zirconate titanate (PZT) films prepared from an electron beam sensitive stock solution were investigated for advanced stage applications in sub 50-nm patterned systems. The required electron beam dose for the direct-patterning of PZT precursor films was 4.5 mC/cm^2. The PZT precursor films with pattern size of 500×500 μm^2 were exposed to an electron beam for 2 h and annealed at 400°C for 30 min under an O_2 ambient. After exposure and annealing, values of the remnant polarization and coercive field were 7.0 μC/cm^2 and 97 kV/cm at 10 V, respectively. These results suggest a possible application of PZT films in micro- or nano-electromechanical systems.

Keywords Electron beam metal-organic deposition · Lead zirconate titanate · Direct patterning · Nano lithography

1 Introduction

To apply ferroelectric films to ferroelectric random access memories (FeRAMs), films should be deposited on top of an underlying integrated-circuit. An annealing temperature of higher than 450°C can induce thermal degradation within Al–Si interconnect on the underlying integrated-circuit [1]. The low temperature crystallization of the ferroelectric films becomes an important issue below an annealing temperature of 450°C. Drouin et al. [2] reported that it was possible to obtain local heating of a platinum silicide film around 300–450°C using a standard scanning electron microscopy (SEM) system. Maki et al. [3] and Huang et al. [1] also report a low temperature-phase formation of a sol-gel derived PZT film around 400–420°C. Furthermore, electron beam lithography has been considered as a potential alternative to optical lithography for critical level patterning in integrated-circuit manufacturing such as nano-electromechanical systems (NEMS) and FeRAMs [4, 5]. For the development of high-density ferroelectric memories (64 Mbit–1 Gbit), ferroelectric capacitor should be patterned in sub-micron size [4]. These findings motivated us to investigate an alternative method for low temperature deposition of direct-patterned PZT films of sub 50-nm width via electron beam sensitive stock solutions using SEM without an electron beam resist or dry etching procedure.

2 Experimental procedure

The starting precursors for the electron beam-induced production of PZT films were the lead (2-ethylhexanoates)$_2$, zirconyl (2-ethylhexanoate)$_2$, and titanium(n-butoxide)$_2$(2-ethylhexanoate)$_2$. These were dissolved in a hexane solvent. The atomic ratio of Zr/Ti was fixed as 52/48 and the molar concentration of the electron beam sensitive stock solution was 0.4 M. The PZT precursor films were spin-coated for 30 s on Pt(111)/Ti/SiO_2/Si(100) substrates with 2×2 cm^2 dimension. Electron beam exposure on spin-coated PZT precursor films was performed by using a Raith e_line e-beam writer with an acceleration voltage of 10 kV for sub 50-nm direct-patterned PZT films. For 500×500-μm^2 direct-

H.-H. Park · H.-S. Lee · H.-H. Park (✉)
Department of Ceramic Engineering, Yonsei University,
134, Shinchon-dong, Seodaemoon-ku,
Seoul 120-749, South Korea
e-mail: hhpark@yonsei.ac.kr

X. Zhang · R. H. Hill
4D Labs and Department of Chemistry, Simon Fraser University,
8888 University Drive,
Burnaby, BC V5A 1S6, Canada

patterned PZT films, an FEI Strata 235 SEM with an acceleration voltage of 10 kV was used and the ferroelectric and dielectric properties were measured. Finally, the electron beam with an acceleration voltage of 5 kV at the 4B1 beam line of Pohang Accelerator Laboratory (PAL) was used for millimeter-scaled films to monitor the compositional evolution with the annealing of the e-beam exposed sample by in-situ photoemission spectroscopy (PES) measurements and to obtain X-ray diffraction (XRD) results. Even though the PZT precursor films were exposed to three different electron beams, the exposed dose was identical: 4.5 mC/cm^2. After exposure of the spin-coated PZT precursor film to the electron beam, the latent image was developed with hexane to yield a negative pattern. The patterned film was annealed at 400°C for 30 min under an O_2 ambient to complete the phase formation with a perovskite structure. The thicknesses of spin-coated, electron beam exposed, and after 400°C-annealed PZT films were around 250, 160, and 150 nm, respectively by ellipsometer measurement. A 150-nm-thick Pt top electrode with a 60-μm radius was sputter-deposited to measure the ferroelectric and dielectric properties of the film.

3 Results and discussion

Changes in the chemical bonding state of the PZT precursor film were monitored after a 2 h electron beam exposure and an annealing treatment from 100°C to 400°C with an interval of 100°C by in-situ PES measurements. Some of the resultant Pb 4f spectra are given in Fig. 1. The PES spectrum of Pb 4f could be fitted to two spin-orbit doublets, which suggests two chemical bonding states: one at Pb $4f_{7/2}$= 138.1 eV and Pb $4f_{5/2}$=143.0 eV, and the other at Pb $4f_{7/2}$= 140.2 eV and Pb $4f_{5/2}$=145.3 eV. The former component was identified as a Pb-O bond [6]. The upward shift of approximately 2.2 eV in the binding energy from one doublet to the other can be ascribed to a Pb–OC bond in the Pb starting precursor, because the Pb precursor was composed only of oxygen and carbon. A similar chemical shift in the Pb $4f_{7/2}$ binding energy was observed with Pb–OS in $PbSO_4$, 2.0 eV from Pb–O [7], due to the similar covalent characteristics of sulfur and carbon with Pb and oxygen. As shown in Fig. 1(b), the doublet peak of Pb–OC was much reduced because the Pb starting precursor was decomposed. Moreover, the doublet peak of Pb-OC had completely vanished after annealing at 400°C (Fig. 1(c)). The Pb 4f peak of Pb–O in the PZT film is given in Fig. 1(d) after annealing at 650°C under an O_2 ambient as a reference. The phase formation of the PZT precursor films was found to be completed after electron beam exposure for 2 h and annealing at 400°C. This was also confirmed by XRD measurements. XRD patterns of direct-patterned PZT films deposited on Pt(111)/Ti/SiO_2/Si(100) substrate are

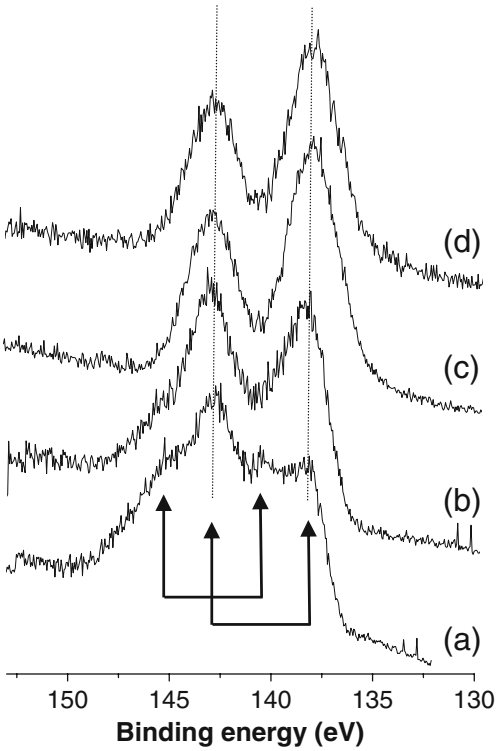

Fig. 1 Evolution of Pb 4f photoemission spectra (**a**) before and after (**b**) electron beam exposure for 2 h and (**c**) subsequent *in-situ* annealing at 400°C or (**d**) subsequent ex-situ annealing at 650°C under an O_2 ambient as a reference

given in Fig. 2. It was only with electron beam exposure of the PZT precursor films for 2 h (Fig. 2(a)) that the films were partially crystallized with a preferred <111> orientation due to (111) plane matching with Pt substrate [8]. Jeyakumar et al. [9] and Saifullah et al. [10] report that an exposure of electron beam sensitive precursor films to an electron beam results in the cleavage of organic ligands from the central metal atom and converts the metal atom to a metal oxide. In our case, the oxygen content was enough for the metal to convert to a metal oxide during the electron beam exposure because the ratio of metal (Pb, Zr, and Ti) to oxygen was 1 to 5 in the PZT starting precursors. After an electron beam exposure for 2 h and subsequent annealing at 400°C for 30 min under an O_2 ambient, the intensity of the (111) diffraction peak increased as shown in Fig. 2(b). However it has been well known that (111)-oriented $PbPt_x$ alloy could be formed in a low temperature reducing atmosphere and act as a seed for the formation of (111)-oriented PZT [11–13]. To check the formation of interfacial $PbPt_x$ alloy, direct-patterned PZT film of 500×500 μm^2 pattern size by an FEI Strata 235 SEM after anneal at 400°C for 30 min under an O_2 ambient was etched using hydrofluoroboric acid [11]. XRD measurements were carried out before and after hydrofluoroboric acid treatments and energy dispersive spectrometry (EDS) analysis

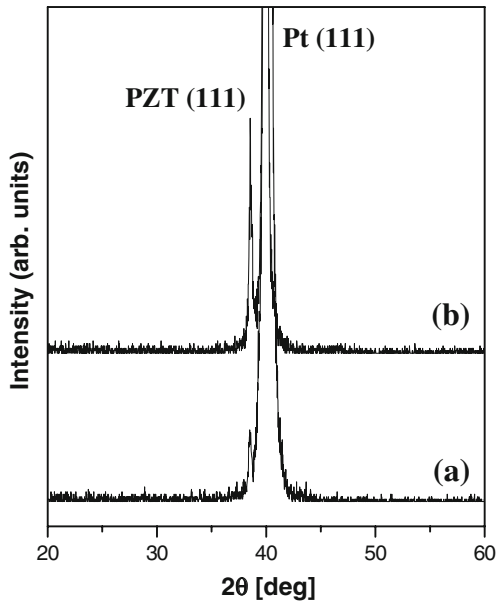

Fig. 2 XRD spectra of direct-patterned PZT films after (**a**) electron beam exposure for 2 h and (**b**) subsequent annealing at 400°C for 30 min under an O_2 ambient

was done on the etched region of the pattern. Figure 3 represents the EDS analysis result and an inset corresponds to the XRD results. As shown in the figure, the intensity of the PZT(111) diffraction peak was reduced much but still existed even after etching of the PZT with hydrofluoroboric acid and the remained peak should be indexed to (111) diffraction of $PbPt_x$ [11]. The EDS analysis result obtained after acid-etched 500×500 μm^2 pattern showed that some Pb was still observed with major Pt. From these results, it could be concluded that through the 400°C-annealing of e-beam treated PZT precursor film for 30 min under an O_2 ambient, (111)-oriented PZT film was synthesized with the presence of interfacial (111)-oriented $PbPt_x$ alloy in case of Pt(111) substrate.

Figure 4 displays the hysteresis loops of the direct-patterned PZT films with pattern size of 500×500 μm^2 under applied voltages of 8, 10, and 15 V using a RT66A ferroelectric tester. The 160 nm thick e-beam exposed PZT precursor film for 2 h did not show a ferroelectric property as shown in Fig. 4(a). This paraelectric behavior of the film may indicate that the crystallization of PZT film with a perovskite structure was not complete, as shown in the Fig. 2(a). However, after the subsequent annealing at 400°C for 30 min under an O_2 ambient, the 150 nm thick PZT film exhibited a well-defined hysteresis loop, typical of ferroelectric behavior (Fig. 4(b)). The remnant polarization (P_r) and coercive field (E_c) values were measured as 7.0 $\mu C/cm^2$ and 97 kV/cm at 10 V, respectively. The P_r value is somewhat small in comparison with that of the PZT films prepared by sol-gel technique [14]. The measured smaller P_r might be associated with low crystalline quality and small grain size due to low annealing temperature, rough interface and possible interfacial mixing between ferroelectric layer and electrode by electron beam bombardment, generated depolarization field, and so on [15–17]. However, the P_r value is somewhat comparable to the value obtained from direct-

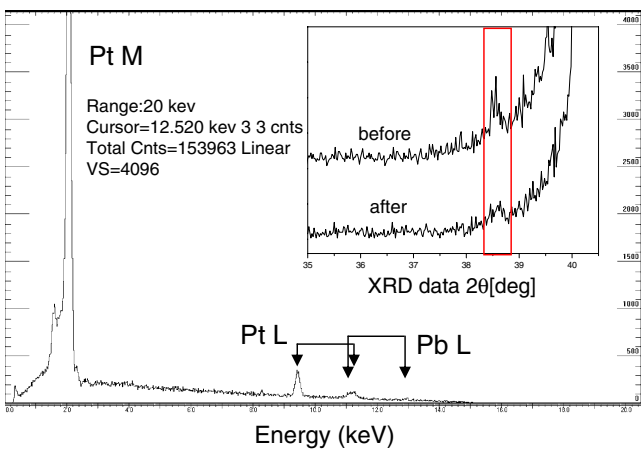

Fig. 3 EDS analysis result on the etched region of direct-patterned PZT film of 500×500 μm^2 size with hydrofluoroboric acid (the inset corresponds to XRD spectra of the direct-patterned PZT film before and after the etching treatment)

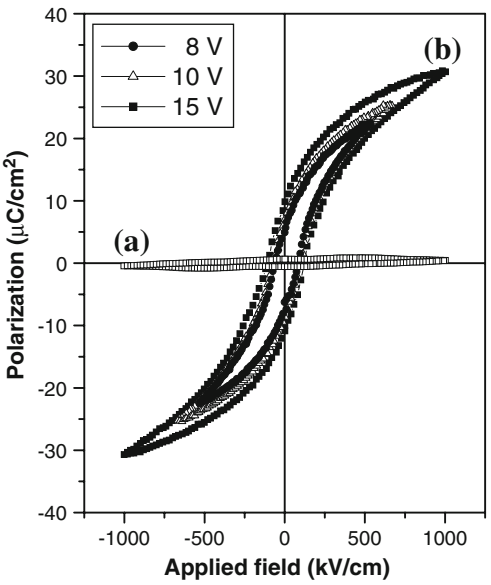

Fig. 4 Ferroelectric hysteresis loops of direct-patterned PZT films after (**a**) electron beam exposure for 2 h and (**b**) subsequent annealing at 400°C for 30 min under an O_2 ambient

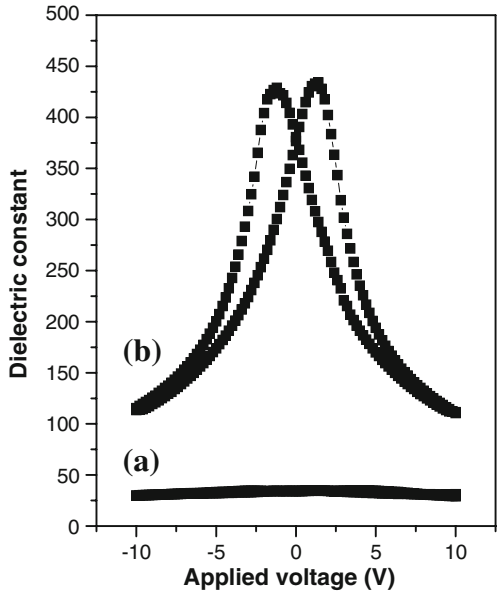

Fig. 5 The voltage dependence of dielectric constants for direct-patterned PZT films after (**a**) electron beam exposure for 2 h and (**b**) subsequent annealing at 400°C for 30 min under an O_2 ambient

patterned PZT film formed using a photosensitive stock solution [18].

The capacitance–voltage (C–V) characteristics of the direct-patterned PZT films with pattern size of 500× 500 μm^2 with an applied voltage range from −10 to 10 V at 1 MHz are given in Fig. 5. As shown in Fig. 5(a), the PZT film exposed to an electron beam for 2 h did not show a butterfly loop while a butterfly loop and two maxima of voltage response peaks with a coercive field were observed with the subsequently annealed PZT film at 400°C for 30 min under an O_2 ambient, as shown in Fig. 5(b). The value of the dielectric constant was 434 for this PZT film which is comparable with reported data on PZT films [19, 20].

SEM micrographs of sub-micron and sub 50-nm direct-patterned PZT films are given in Fig. 6. After the PZT precursor films were exposed with a dose of 4.5 mC/cm^2 using a FEI Strata 235 SEM or Raith e_line e-beam writer, the exposed PZT precursor films were developed by hexane-rinsing to reveal the negative pattern. The relatively bright area corresponds to direct-patterned PZT films and the relatively dark area corresponds to a Pt substrate. Based on Fig. 6, we conclude that the electron beam dose (4.5 mC/cm^2) to which the PZT precursor films were exposed was sufficient for the completion of structural arrangements including local networking. Together, our results indicate that direct-patterned PZT films can be realized using an electron beam sensitive stock solution for NEMS and FeRAMs applications.

4 Conclusions

In summary, we have demonstrated an electron beam resist-free fabrication technique to deposit sub 50-nm direct-patterned PZT films at low temperature. The PZT precursor film exposed to an electron beam for 2 h did not have ferroelectric properties. However, after subsequent annealing at 400°C for 30 min under an O_2 ambient, PZT film with perovskite structure was synthesized with interfacial (111)-oriented $PbPt_x$ alloy on Pt(111) substrate. The direct-patterned PZT films with pattern size of 500× 500 μm^2 exhibited well-defined hysteresis loops and butterfly loops for C-V curves. This electron-beam induced sub 50-nm direct-patterning technology of PZT ferroelectric films can therefore be effectively adopted to fabricate sub 50-nm-patterned systems.

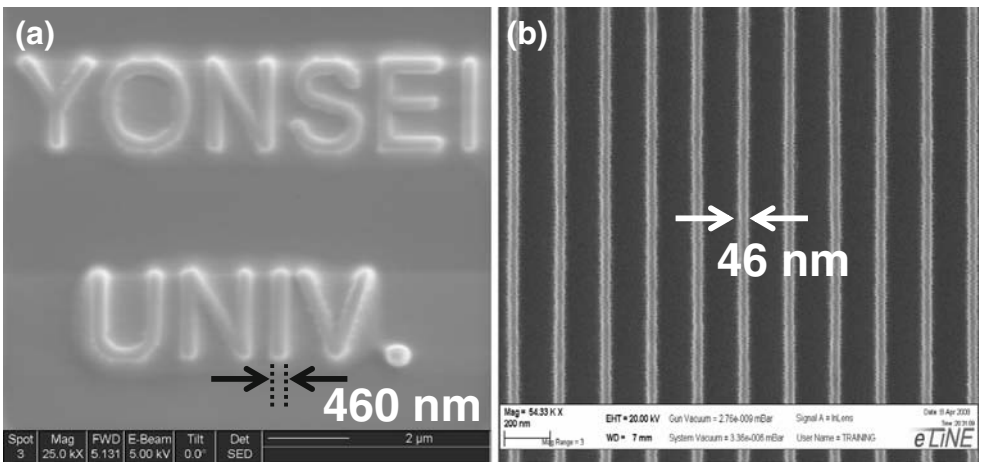

Fig. 6 SEM micrographs of direct-patterned PZT films using an electron beam sensitive stock solution by (**a**) an FEI Strata 235 SEM or (**b**) a Raith e_line e-beam writer

Acknowledgements This work was supported by the Korea Research Foundation Grant funded by the Korean Government (MOEHRD, Basic Research Promotion Fund) (KRF-2006-311-D00636). The experiments performed at the PLS were supported in part by the MOST and the POSTECH.

References

1. Z. Huang, Q. Zhang, R.W. Whatmore, J. Appl. Phys **85**, 7355 (1999). doi:10.1063/1.369362
2. D. Drouin, J. Beauvais, R. Lemire, E. Lavallée, R. Gauvin, M. Caron, Appl. Phys. Lett **70**, 3020 (1997). doi:10.1063/1.118736
3. K. Maki, N. Soyama, K. Nagamine, S. Mori, K. Ogi, Mater. Res. Soc. Symp. Proc **688**, C1.4.1 (2002)
4. M. Alexe, C. Harnagea, D. Hesse, U. Gösele, Appl. Phys. Lett **75**, 1793 (1999). doi:10.1063/1.124822
5. K. Malladi, C. Wang, M. Madou, Carbon **44**, 2602 (2006). doi:10.1016/j.carbon.2006.04.039
6. T.J. Zhu, L. Lu, J. Appl. Phys **95**, 241 (2004). doi:10.1063/1.1631750
7. D. Briggs, M.P. Seah, *Practical surface analysis*, 2nd edn. (Wiley, New York, 1990), p. 623
8. H.-H. Park, H.-H. Park, R.H. Hill, Appl. Surf. Sci **237**, 427 (2004). doi:10.1016/j.apsusc.2004.06.103
9. A. Jeyakumar, C.L. Henderson, P. Roman, S. Suh, J. Vac. Sci. Technol. B **21**, 3157 (2003). doi:10.1116/1.1624250
10. M.S.M. Saifullah, K.R.V. Subramanian, E. Tapley, D.-J. Kang, M.E. Welland, M. Butler, Nano Lett **3**, 1587 (2003). doi:10.1021/nl034584p
11. Y.L. Tu, S.J. Milne, J. Mater. Res **10**, 3222 (1995). doi:10.1557/JMR.1995.3222
12. A.D. Cristoforo, P. Mengucci, G. Majni, F. Leccabue, B.E. Watts, G. Chiorboli, Mater. Sci. Eng **B47**, 263 (1997). doi:10.1016/S0921-5107(97)00044-5
13. Z. Huang, Q. Zhang, R.W. Whatmore, J. Mater. Sci. Lett **17**, 1157 (1998). doi:10.1023/A:1006548417377
14. F. Yang, W.D. Fei, Q. Sun, J. Mater. Process. Technol **209**, 220 (2009). doi:10.1016/j.jmatprotec.2008.01.042
15. A.Q. Jiang, Y.Y. Lin, T.A. Tang, J. Appl. Phys **101**, 056103 (2007). doi:10.1063/1.2436921
16. A.Q. Jiang, Y.Y. Lin, T.A. Tang, J. Appl. Phys **101**, 104105 (2007). doi:10.1063/1.2733640
17. A.Q. Jiang, Y.Y. Lin, T.A. Tang, J. Appl. Phys **102**, 074118 (2007). doi:10.1063/1.2795572
18. G.Y. Kang, S.-W. Bae, H.-H. Park, T.S. Kim, Appl. Phys. Lett **88**, 042904 (2006). doi:10.1063/1.2168261
19. E.B. Araújo, J.A. Eiras, J. Mater. Sci. Lett **18**, 1679 (1999). doi:10.1023/A:1006673615512
20. Q. Zou, H.E. Ruda, B.G. Yacobi, K. Saegusa, M. Farrell, Appl. Phys. Lett **77**, 1038 (2000). doi:10.1063/1.1289060